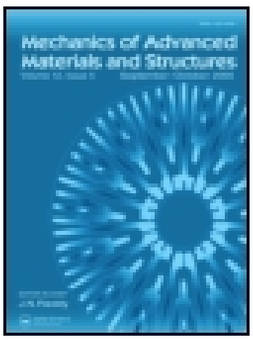

Mechanics of Advanced Materials and Structures

ISSN: 1537-6494 (Print) 1537-6532 (Online) Journal homepage: http://www.tandfonline.com/loi/umcm20

Best pattern for placement of piezoelectric actuators in classical plate to reduce stress concentration using PSO algorithm

Javad Jafari Fesharaki, Seyed Ghasem Madani & Sa'id Golabi

To cite this article: Javad Jafari Fesharaki, Seyed Ghasem Madani & Sa'id Golabi (2018): Best pattern for placement of piezoelectric actuators in classical plate to reduce stress concentration using PSO algorithm, Mechanics of Advanced Materials and Structures, DOI: 10.1080/15376494.2018.1472332

To link to this article: https://doi.org/10.1080/15376494.2018.1472332

MECHANICS OF ADVANCED MATERIALS AND STRUCTURES
2018, VOL. 0, NO. 0, 1–11
https://doi.org/10.1080/15376494.2018.1472332

Taylor & Francis
Taylor & Francis Group

ORIGINAL ARTICLE

Best pattern for placement of piezoelectric actuators in classical plate to reduce stress concentration using PSO algorithm

Javad Jafari Fesharaki[a,b], Seyed Ghasem Madani[c], and Sa'id Golabi[c]

[a]Department of Mechanical Engineering, Najafabad Branch, Islamic Azad University, Najafabad, Iran; [b]Modern Manufacturing Technologies Research Center, Najafabad Branch, Islamic Azad University, Najafabad, Iran; [c]Department of Mechanical Engineering, Faculty of Engineering, University of Kashan, Kashan, Iran

ABSTRACT

The purpose of this article is using piezoelectric actuators to reduce stress concentration factor in classic plates under tensile force. There are three classic plates in this study including plates with hole, notched plates, and filleted plates. Here we look for optimal models for placement of the introduced piezoelectric actuators at different ratios of stiffness to maximize reduction in stress concentration factor. In order to optimize piezoelectric actuators placement, particle swarm optimization algorithm is used. The results show that the location of patches is changed by different values of stiffness ratio (stiffness of plate/stiffness of patches). The findings indicate that the piezoelectric actuators placement models are different for stiffness values at smaller and greater than 1 in classical plates. For stiffness ratios smaller than 1, the patches can reduce the stress directly. However, the actuators follow a certain model in all classic plates at stiffness ratio greater than 1, and reduce stress stream indirectly by affecting the stress stream. The results show that there is a certain model for placement of piezoelectric actuators at any certain stiffness ratio in all classical plates. Three empirical tests have been used to validate the results.

ARTICLE HISTORY
Received 12 January 2018
Accepted 24 March 2018

KEYWORDS
Classical plate; piezoelectric actuators; reduce stress concentration; PSO algorithm; optimization

1. Introduction

Using piezoelectric materials in structures has been studied by different scientists for control of stress, form of structure, and buckling during recent years. This is also the case for reservoirs under pressure. For example, the walls of these reservoirs in which there is a hole with a nozzle, the stress concentration is created. This stress concentration can be controlled by embedding an extra sheet around the hole as reinforcement. There is also a high level of tension at connection points of reservoir stands to the wall, which is controlled adding the sheet between the reservoir and the base. In cases where the reservoir is subjected to additional loads such as earthquakes or winds, these points of tension concentration may cause the problem. Increasing the thickness of the reservoir wall to avoid the effect of the concentration of stress is expensive for this field of industry. However, according to the ASME code, raising the reinforcement or increasing the whole wall thickness of the reservoir are the only solutions at the moment. Using piezoelectric cells to control the additional tensions and, in general, the local stresses can be an applicable solution to control stress concentrations. More examples can be found in other industries such as vehicles industry. Due to high cost of piezoelectric materials, researchers look for optimal use of piezoelectric in structures. Therefore, using particle swarm optimization (PSO) algorithm they have searched for finding the optimal placement of piezoelectric actuators on structures to reduce costs at maximum level and to reach best efficiency of piezoelectric actuators. Some of these studies on optimization of piezoelectric actuators placement are available in former literatures [1]–[3].

Roy et al. [4] investigated an optimal control of vibrations of a cylindrical composite shell. Using genetic algorithm, they extracted the required voltage to control the shell vibrations and identified the best piezoelectric cells placement on shell. Mehrabian and Yousefi-Koma [5] showed a new method for best piezoelectric cells placement on smart structures under vibrations. As an example of their analysis, they put a blade that can be a part of an airplane under vibrations and determined the best location for piezoelectric cells placement on it. Dadfarnia et al. [6] worked on control of vibrations of a robot's arm. They considered the robot arm as a one-end blocked beam on which a piezoelectric cell was placed. Mukherjee and Chaudhuri [7] worked on active control of a column under vibrations. They considered effect of vertical force exerted on column and tried to propose numerical solution to control vibrations. Jadhav et al. [8] explored control of vibration of functionally graded material (FGM) material by piezoelectric materials displaced at both sides of the plate. Guo et al. [9] studied vibration control of a sandwich sheet using piezoelectric materials. Guo et al. [10] investigated the optimal placement of piezoelectric operators in a sandwich plate in order to control vibrations of the structure.

Kumar et al. [11] investigated static and dynamic analysis of a cylindrical shell. They tried to propose finite element method (FEM) model for cylindrical shell on which piezoelectric cells could be located on different positions; also it was

CONTACT Javad Jafari Fesharaki Jafari@pmc.iaun.ac.ir Department of Mechanical Engineering, Najafabad Branch, Islamic Azad University, Najafabad, Iran.
Color versions of one or more of the figures in the article can be found online at www.tandfonline.com/umcm.

under mechanical, electric, and thermal fields. Yao et al. [12] explored healthy welding joints by means of piezoelectric materials. They employed a piezoelectric element as driving unit and another piezoelectric structure as sensor and examined healthy welded joints by the generated wave. Tao et al. [13] examined the integrity of bolted connections using piezoelectric materials. Wu and Wang [14] examined controlling lamination of a plate by piezoelectric materials and using FEM. Then they studied a beam on which a hole was arranged and it was under dynamic loading. They analyzed stress concentration under dynamic loading by doing empirical test and placement of piezoelectric cells as sensor near the crack. Then, they controlled growth of the crack by the aid of reverse phenomenon of piezoelectric cells by placement of piezoelectric cells near to the crack. Kurata et al. [15] diagnosed defects in steel structures using piezoelectric materials.

Correia et al. [16] studied on optimization of piezoelectric cells placement on a composite plate. They integrated FEM with simulated annealing optimization technique and thereby they extracted an optimum placement of piezoelectric cells to achieve maximum quantity of bulking load. Daraji and Hale [17] studied optimal placement of actuators and sensors to control the active vibration. They used genetic algorithm and by updating mode shape and natural frequencies investigated the global optimal solution. Fey et al. [18] investigated the response of electrical and mechanical strain of piezoelectric structures. Nguyen et al. [19]–[21] worked on controlling form of a composite plate. They primarily filled total surface of the plate with piezoelectric cells. Then given various shapes for plate deformation, using voltage for piezoelectric cells as well as employing ordinary least square method they tried to minimize the related error between the given deformation and real deformation of the plate. As a result, piezoelectric cells, which did not need exertion of voltage in optimization process, were deleted and the obtained rest cells indicated optimal level of piezoelectric cells to achieve designated form for plate. Kang et al. [22], [23] studied controlling form of a plate with synchronous distribution of material and voltage. The goal of their study was also to exert voltage to piezoelectric cells for which they could exert favorable shape on plate. To this end, they considered constraint of minimum energy and minimum materials. Likewise, they research on effect of existing adhesive and electrode layer in piezoelectric cells. They coated the surface of the plate by a piezoelectric layer and then controlled it by changing the quantity of exerted voltage to achieve designated form of plate. The important point of their work was allowing exertion of reverse voltage to piezoelectric cells; as a result, piezoelectric cells can be separately under positive or negative strain.

Sensharma et al. [24] investigated for the first time the control of tension by a device which can produce strain. They used a plate with a hole and explained that the device producing strain can be a piezoelectric plate or shape memory alloys. To investigate that, they employed FEM, and to produce applied strain, they added it as the heat to the equations. They concluded that in the case of possessing right tools to apply strain around the hole, it can reduce the stress concentration in dangerous places. Shah et al. [25], [26] observed the reduction of the stress concentration in plate with hole using piezoelectric cells. Their main idea was that in order to reduce the stress concentration around the holes, it was not necessary to place the piezoelectric cells in stress concentration points. Instead, the cell should be placed in other points usually yielding zero stress. They expressed that the piezoelectric cells should control the stress stream in the piece rather than controlling the stress amount in maximum stress points, so that the stress would be reduced at dangerous points by making stress uniform. Jafari et al. [27] reviewed impact of ratios of modulus of elasticity and thickness on reduction of stress concentration factor in a plate with cavity using piezoelectric actuators. Using PSO algorithm, Golabi et al. [28] introduced a reference baseline for placement of piezoelectric actuators to reduce stress concentration factor on a plate with cavity. Jafari and Golabi [29] introduced the best model to place the piezoelectric actuators around a hole in a plate in order to reduce stress concentration using the PSO algorithm.

Using piezoelectric actuators, the best models to reduce stress concentration factor have been examined in this study for placement of piezoelectric pieces at different ratios of stiffness around the point with maximum stress concentration in classic plates. The classic plates include plate with hole, notched plate, and filleted plate. A python code has been developed for optimization based on PSO algorithm for Abaqus software. The precision of the given results has been measured by empirical tests.

2. Finite element formulation

In the considered problem, mechanical behavior of the plate has been modeled for a thin plate under tensile force using first-order shear theory in which p, s, and k are assumed as plate displacement elements at any point:

$$\begin{aligned} p(x, y, z) &= p_0(x, y) + z\theta_x(x, y) \\ s(x, y, z) &= s_0(x, y) + z\theta_y(x, y) \\ k(x, y, z) &= k_0(x, y) \end{aligned} \tag{1}$$

where p_0, s_0, and k_0 are plate displacement components at mid-plane of the plate. θ_x and θ_y denote the rotation of element from middle plate along x and y direction respectively. Using FEM formulae, displacement and coordinates inside element for host plate and piezoelectric plate are expressed as follows:

$$x = \sum_{i=1}^{n} H_i x_i, \quad \mathrm{y} = \sum_{i=1}^{n} H_i y_i \tag{2}$$

where n is number of node and H_i is the shape function for elements. The linear equations of piezoelectric cells may also be written for two electric and elastic fields as follows:

$$\sigma = R\varepsilon - aE, \quad D = a^T\varepsilon + pE \tag{3}$$

where σ and ε are stress coefficient and elastic strain, respectively. R, D, a, and P are constants of elastic matrix, electric displacement vector, piezoelectric stress matrix index, and dielectric matrix, respectively. Field vector E is expressed as follows:

$$E = -\Delta\Phi \tag{4}$$

where Φ is exerted electric voltage throughout thickness of piezoelectric actuators. Hamilton's principle has been utilized to solve displacement equation for a plate including piezoelectric actuators. This principle is expressed for an electromechanical

system as follows:

$$\int_{a1}^{a2} \delta(T - U + W_{ext})da = 0 \tag{5}$$

T, U, and W_{ext} denote kinetic energy, potential energy, and work done by external forces, respectively. These parameters are defined as follows:

$$\begin{aligned} T &= \int_V \frac{1}{2}\rho\{\dot{S}\}^T\{\dot{S}\}dV \\ U &= \int_V \frac{1}{2}\left[\{\varepsilon\}^T\{\sigma\} - \{E\}^T\{D\}\right]dV \\ W_{ext} &= \sum_{i=1}^{m_f}\{S\}^T\{F_b\} \end{aligned} \tag{6}$$

$\dot{S}$, ρ, F_b, and m_f are velocity vector, density, vector of external forces, and quantity of exerted forces respectively, and V is volume of structure. Because of considering the static state in this paper, the kinetic energy is considered to have zero value.

3. Particle swarm optimization (PSO) algorithm

PSO, which is also known as bird algorithm, is based on the behavior of birds or fishes group discovered in 1995 by Kennedy and Eberhart [30]. For example, the particle is considered as a bird in a group. The behavior of any particle or bird is based on two parameters: a) its innate intelligence and b) social intelligence of the group to which it belongs. If a bird finds a direction to the food, it causes others to follow that direction immediately even though they are far away from the food.

For optimization by PSO, a fixed number of particles should be considered; for every particle two important parameters are noticed: a) particle location and b) particle speed. Each particle circles in a defined space and memorizes the best place it finds, and then the members of the group begin to communicate the best places discovered to each other. Each member adjusts itself to the place and speed based on the information received. PSO has been developed based on the following models:

1) When a bird finds food (maximum objective function), it communicates immediately its data to the other birds.
2) Other birds tend to fly toward the food (maximum objective function), but they don't move directly. It should be noted that in the optimization process, the other birds may find better foods while flying toward that source of food and then by informing other group's members lead them to fly there.

If supposed that optimization process is followed by maximum value of function $F(x)$ in which x is placed within range $X_l \le x \le X_u$, X_l and X_u are lower and upper boundaries of x, respectively; PSO algorithm will be implemented according to the following steps.

Step 1: The number of particles (birds) is assumed as N. Smaller quantity of particles should be selected for the group in order to reduce number of needed calculations to be done to lead to the answer. However, if the number of group particle selected is too small, particles should do further search to converge toward a same point. Therefore, the time of solving the problem becomes longer, or even the process may unlikely lead to convergent. Usually groups with 20–30 members are considered in this paper.

Step 2: Initially, location of group members is randomly placed within the given range. Thus, one can consider location of group members as $X_1, X_2, \ldots, X_n$.

Location and velocity of jth particle at ith iteration is displayed as X_j^i and V_j^i. Therefore, primary position of members is expressed as $X_1^0, X_2^0, \ldots, X_n^0$. For example, X_2^0 denotes the location of second member at 0th iteration (or primary mode). Then, the objective function for any member is equivalent to $f(x_1^0), f(x_2^0), \ldots, f(x_n^0)$, is calculated.

Step 3: Finding of velocity for all members: All members move toward optimal point by unique velocity. It is supposed at primary mode that all members have zero velocity. Now, iteration number is set as 1 ($i = 1$).

Step 4: Finding two important parameters of jth member at ith iteration:

a) The best value of X_j^i shown by $p_{\text{best},j}$ in fact is the location of highest value of target function $f(x_j^i)$ that has been acquired by jth member in previous iterations.
b) The best value of X_j^i shown by g_{best} is in fact the maximum value of target function that has been acquired by all members in previous iterations.

Step 5: Velocity of jth member in ith iteration is extracted as follows:

$$\begin{aligned} V_j^{(i)} = V_j^{(i-1)} &+ l_1 j_1\left[P_{Best,j} - X_j^{(i-1)}\right] \\ &+ l_2 j_2\left[G_{Best} - X_j^{(i-1)}\right]; \quad j = 1, 2, \ldots, N \end{aligned} \tag{7}$$

In this equation, l_1 and l_2 are rates of individual and social learning of any member and j_1 and j_2 are random values between zero and one. Parameters l_1 and l_2 display important relation among memory of any member and memory of group. Values of l_1 and l_2 are usually both supposed as 2.

Step 6: Location of ith member at jth iteration is derived according to the following formula:

$$X_j^{(i)} = X_j^{(i-1)} + V_j^{(i)}; \quad j = 1, 2, \ldots, N \tag{8}$$

Then, equivalent values of target function are found for any member, i.e., $f(x_1^i), f(x_2^i), \ldots, f(x_n^i)$.

Step 7: Convergence criterion is checked after above steps. If location of all members has approached to a certain value, the solution is converged and if the convergence criterion has not satisfied, this process should be repeated from Step 4. At this phase, the number of iteration is considered as $i = i + 1$ and new values of $p_{\text{best},j}$ and g_{best} are calculated again.

4. Definition of problem

Three plates with length 200 mm, width 100 mm, and thickness of 20 mm have been considered under tensile force of 1 MPa for geometry of problem. The rate of effect by piezoelectric actuators is greater near the cavity, notched, and filleted points on reduction of stress concentration. Thus, a 5 × 5 imaging meshes has been designated for surrounding cavity, notched, and filleted points. Problem geometry and meshing network are shown for piezoelectric actuators placement in Figure 1.

A ratio of stiffness is defined to analyze piezoelectric actuators placement model that is the product of dividing force to

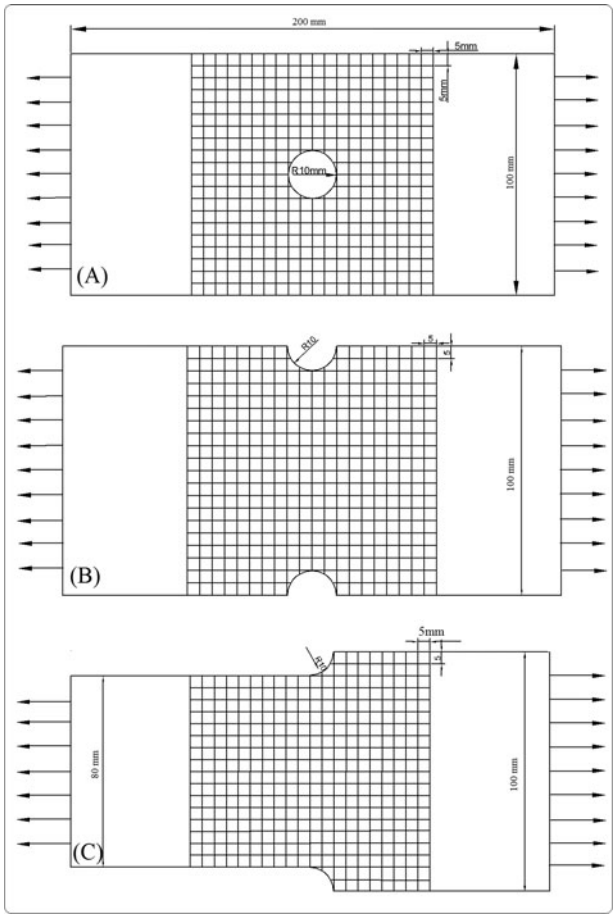

Figure 1. Geometry of problem and virtual meshing network.

piezoelectric actuators and host plate. Ratio of stiffness or Rs is defined as

$$\mathrm{Rs} = \frac{(E \times t)_{\mathrm{Piezo}}}{(E \times t)_{\mathrm{Plate}}} \tag{9}$$

where "E" is the module of elasticity and "t" is the thickness of plate for host plate and piezoelectric patches. It should be noted that the module of elasticity and the thickness of plate have the same behavior to absorb and bear the applied force. For example, if we consider two sticking plate, they will be loaded under tensile force, the plate with a higher thickness or higher module of elasticity, will bear a larger share of the load. The definition of the stiffness ratio for the plate is also based on the ability to withstand the force for the plate and piezoelectric patches.

The optimal model for piezoelectric actuators placement is acquired in values of stiffness ratio greater and smaller than 1 as follows:

$$\mathrm{Rs} = 10, 4, 3, 2, 1, \frac{1}{2}, \frac{1}{3}, \frac{1}{4}, \frac{1}{10} \tag{10}$$

A python code for abaqus software has been developed in order to simulate and define the problem using the PSO algorithm. To find the optimized voltage and the best location for piezoelectric structures placement around the cavity, notched, and filleted points, the PSO is used for any stiffness ratio. To find the optimal voltage and best location for piezoelectric structures around the cavity, PSO algorithm is utilized at any stiffness ratio. In this paper, using the PSO optimization algorithm, the best locations for placement of piezoelectric operators are utilized in order to reach the highest reduction in the stress concentration factor on the page. Using PSO optimization algorithm, the best position identifies and piezoelectric operator is located at that point, then the optimal position will be found and this will continue until we reach 12% of the piezoelectric operators. To this end, percentage of occupied surface area by piezoelectric structures and value of stiffness to code ratio are given initially. With respect to meshing region, PSO algorithm finds the best point for piezoelectric pieces around the cavity. Flowchart of execution of algorithm and PSO optimization is displayed in Figure 2. It should be noted that the algorithm converges when the patches do not change after 100 iterations.

5. Discussion and analysis

The optimal pattern for piezoelectric actuators placement in three plates with hole, notched, and filleted structures have been examined by execution of developed python. The results for each plate is presented as

5.1. *Plate with hole*

The optimal model of piezoelectric actuators placement around the hole is shown for stiffness ratios greater than 1 in Figure 3. The piezoelectric actuators located at left and right of hole at stiffness ratio 1 and they have been placed longitudinally in respective of plate.

It is observed that, if the stiffness ratio increases, the number of actuators is reduced longitudinally along the plate and it is added to number of them at transversal along the plate. So, the actuators have been placed transversally along the plate at stiffness ratio 10. The piezoelectric actuators placement model is shown at stiffness ratios smaller than 1 in Figure 4, where actuators are located above and under the cavity and placed transversally along the plate. Reduction of stress concentration factor is observed at different number of piezoelectric structures for stiffness ratios greater than 1 around the hole in Figure 5. At stiffness ratio 1, the maximum reduction in stress concentration is observed. By increasing stiffness ratio and approaching to 10, the rate of reduction is decreased in stress concentration factor.

Reduction of stress concentration factor is shown for stiffness ratio less than 1 in Figure 6. It is observed that stiffness ratios 1/2 and 1/10 indicate the maximum and minimum reductions in stress concentration factor, respectively. The longitudinal stress around the cavity is shown at stiffness ratios greater and smaller than 1 in Figures 7 and 8. It is seen in Figure 7 that the maximum stress has occurred in stiffness ratio 10 at angle 90°. However, the maximum stress has been transferred to the point at angle about 60° in other ratios.

5.2. *Notched plate*

The optimal model of piezoelectric actuators placement around the notched area in plate is shown for stiffness ratio greater than 1 in Figure 9. It is seen that the piezoelectric actuators are located at left and right of the notched plate with stiffness ratio 1 and they have been placed longitudinally in respective of plate. Following the rise of stiffness ratio, numbers of piezoelectric

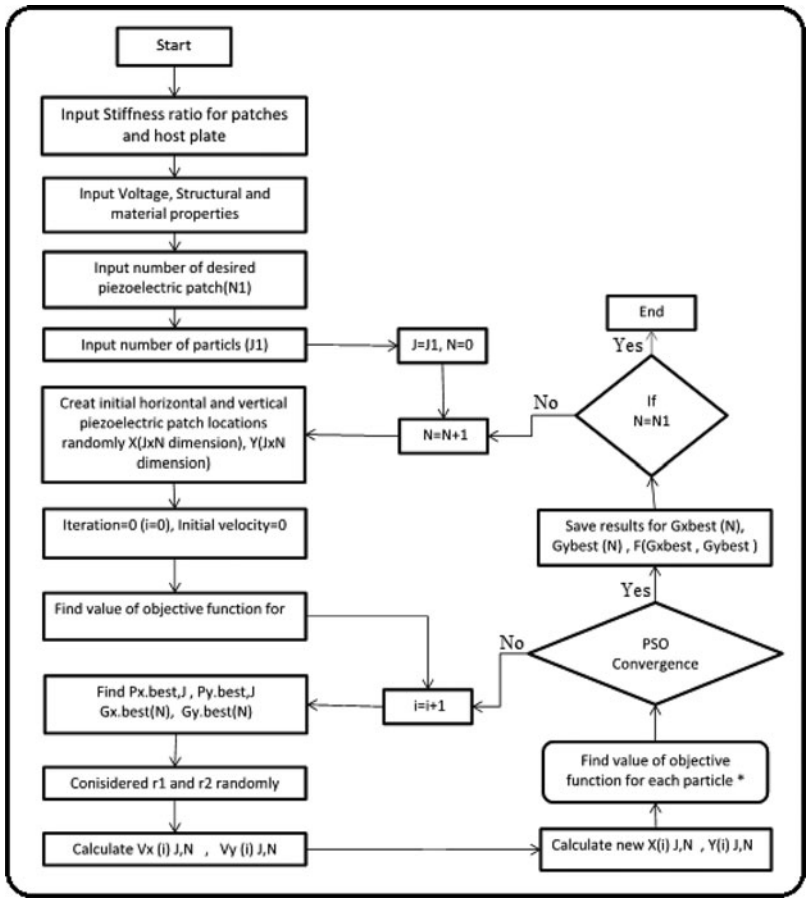

Figure 2. Flowchart of PSO for consideration problem.

actuators are reduced at right and left sides of the notched areas and it was added to their quantity at transversal axis of plate. The piezoelectric actuators have been totally placed transversally at stiffness ratio 10.

The optimal model of piezoelectric actuators placement is shown for stiffness ratios greater than 1 in Figure 10. It is observed that the actuators are located above the notched point and they are placed transversally to the plate.

Reduction percent of stress concentration factor is displayed for stiffness ratios greater than 1 in Figure 11. We observe that the maximum reduction of stress is about 44% at stiffness ratio 1 and as stiffness ratio increases, the reduction rate is decreased in stress concentration factor and it approaches to about 23% at Rs = 10.

Reduction of stress concentration factor is shown for stiffness ratios smaller than 1 in Figure 12. It is seen that as stiffness ratio reduces, the percent of reduction is also decreased in stress concentration factor.

The longitudinal stress is shown around notched area for various stiffness ratios in Figures 13 and 14. It is observed in Figure 13 that the diagrams include peaks at angles about 10 and 65° at stiffness ratios 2, 3, and 4 and maximum stress takes place at angle 90° for all modes.

5.3. *Filleted plate*

The optimal model of piezoelectric actuators placement around the fillet area is indicated at stiffness ratios greater than 1 in Figure 15. It is observed in stiffness ratio 1 that the piezoelectric actuators are placed at left and right ends of filleted area and longitudinally toward plate. Following the rise in stiffness ratio, the number of piezoelectric actuators is reduced longitudinally to plate while it is added to their number at transversal axis. Placement of piezoelectric actuators is shown at stiffness ratios smaller than 1 in Figure 16. It is seen that the piezoelectric actuators have been placed above the filleted area and transversally toward plate.

Percent of reduction in stress concentration factor has been shown in Figure 17 for stiffness ratios greater than 1 in various percent of piezoelectric actuators. We observe in stiffness ratio 1, maximum percent of reduction in stress is seen about 50%. As stiffness ratio increases, reduction percent of stress concentration factor is decreased so that percent of reduction in stress concentration factors approaches to about 23% at stiffness ratio 10.

Percent of reduction in stress concentration factor is indicated for stiffness ratio smaller than 1 in Figure 18. It is observed that following the decrease in stiffness ratio, percent of reduction in stress concentration ratio is decreased.

Longitudinal stress is shown around the filleted area at different stiffness ratios in Figures 19 and 20. It is observed in Figure 19 that at Rs = 1, maximum stress concentration is located about angle 80° and it is about 65° at Rs = 2. Stress concentration takes place at angle 90° in stiffness ratios 3 and 4 and stress concentration occurs in approximately angle 65° again at Rs = 10. In Figure 20, stress concentration takes place in all stiffness ratios at about angle 78°.

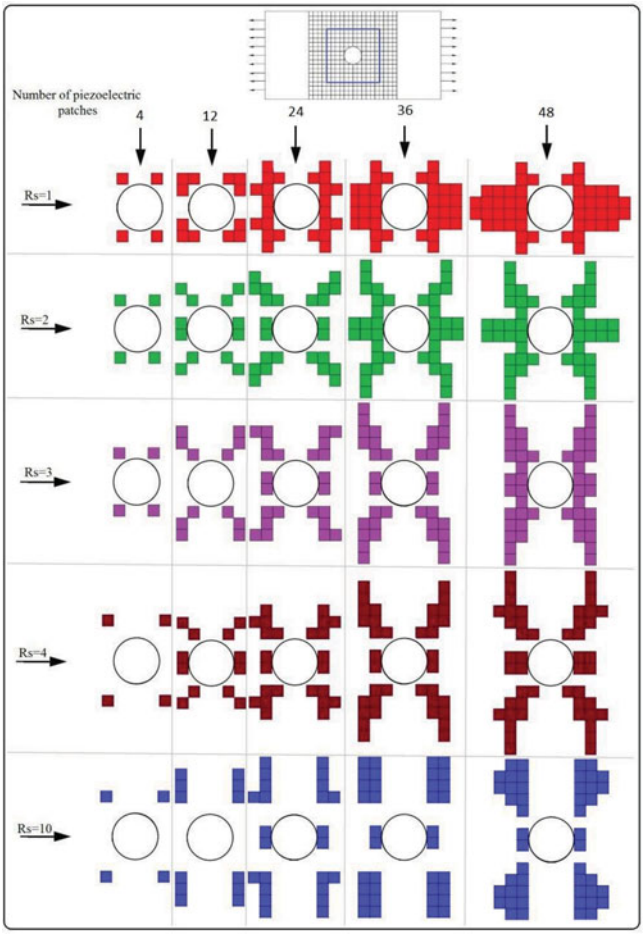

Figure 3. The best pattern of piezoelectric actuators placement around the hole for Rs $\geq$ 1.

It is concluded from the previous sections that if we intend to use stiffness ratios greater than 1 between piezoelectric actuators and host plate, the smaller stiffness ratios should be utilized to achieve maximum reduction in stress concentration factor. If we like using stiffness ratio smaller than 1, we should employ greater ratios to achieve maximum reduction in stress concentration factor. In all three plates, the actuators have been placed longitudinally toward plate in stiffness ratio 1. As stiffness ratio increases, number of piezoelectric actuators is reduced longitudinally in plate while it is increased transversally toward plate.

6. Results of validation

The results of three tests have been considered for validation of any plate with cavity, notched, and filleted plate in any test in this paper. With respect to the designated dimensions for classic plates in Figure 1, plates were made of aluminum and Pzt-4 type of piezoelectric. The strain gauge is located in the longitudinal direction of the plate, and it is precisely in the place in which there is the maximum stress concentration on the plate, i.e., up and down the hole. The results of Tables 1–3 all indicate the accuracy of the finite element responses and the accuracy of the piezoelectric operator's performance in a laboratory test. Figure 21 shows the schematic and test

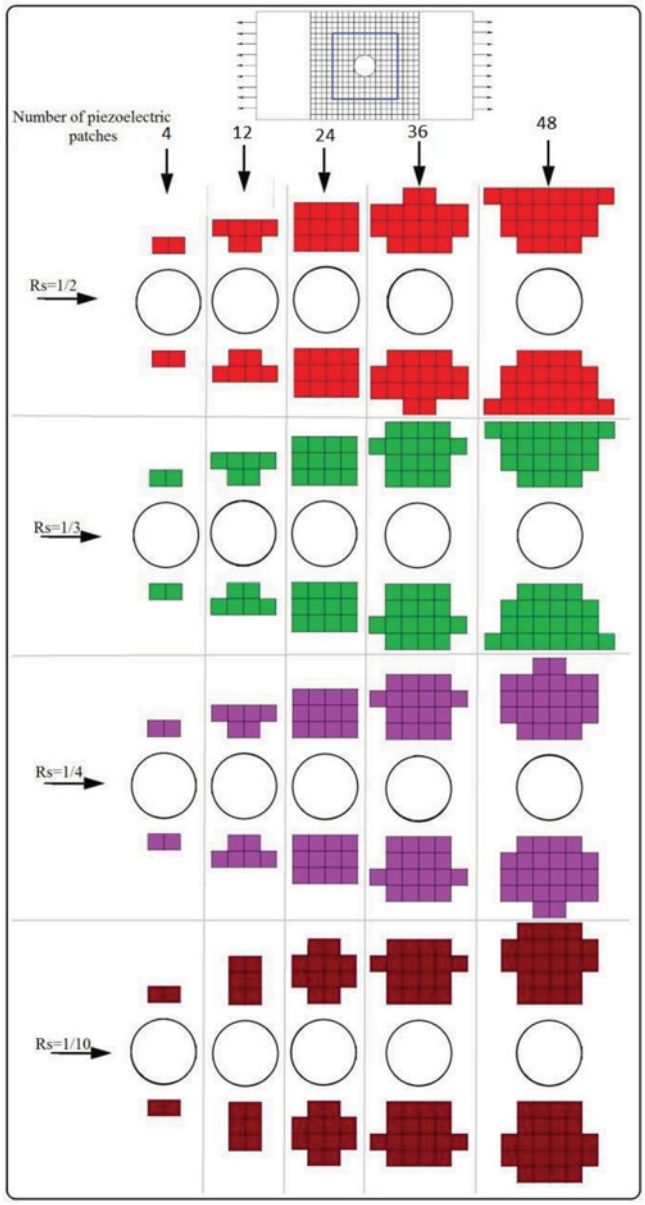

Figure 4. The best pattern of piezoelectric actuators placement around the hole for Rs $<$ 1.

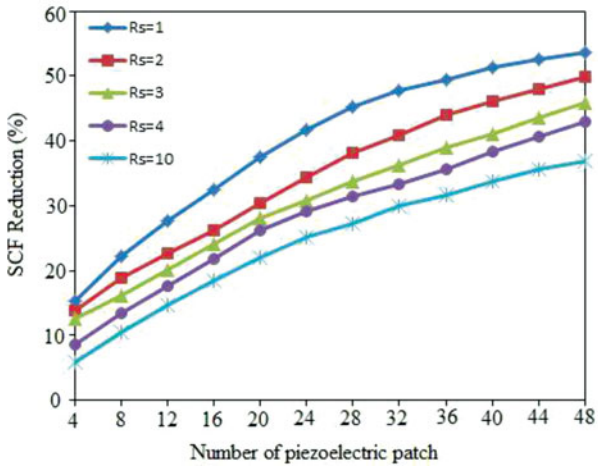

Figure 5. Effect of stiffness ratio on stress concentration reduction for Rs $\geq$ 1.

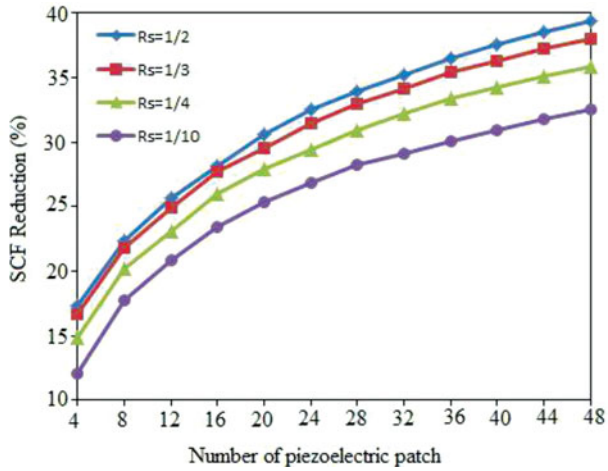

Figure 6. Effect of stiffness ratio on stress concentration reduction for Rs < 1.

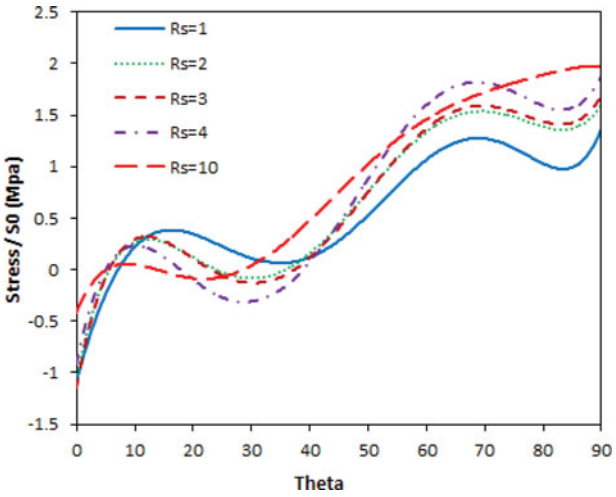

Figure 7. Longitudinal stress around the hole for Rs ≥ 1.

setup for experimental tests. The rate of strain is recorded on host plate by strain-gauges by induction of electric voltage to piezoelectric actuators in empirical test and then the precision of the given test is examined by comparing numerical and empirical results given in Tables 1–3. As is identified from

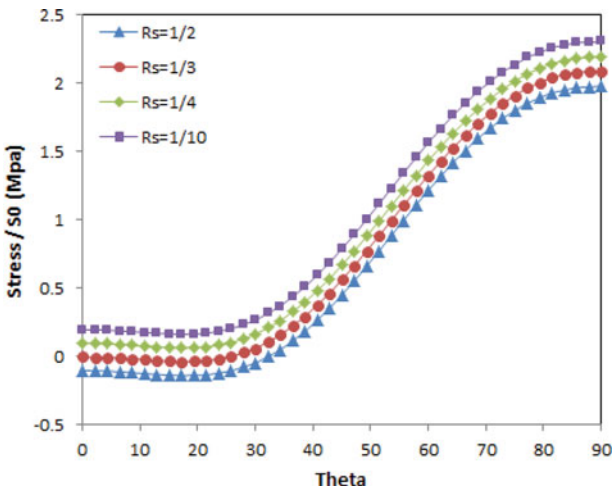

Figure 8. Longitudinal stress around the hole for Rs < 1.

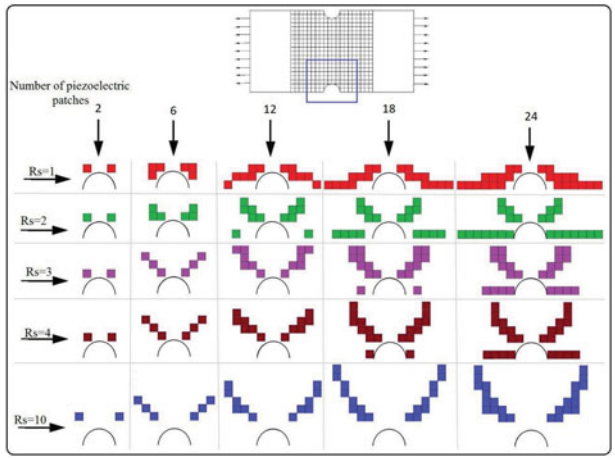

Figure 9. The best pattern of piezoelectric actuators placement around the notched for Rs ≥ 1.

results of Tables 1–3, the empirical results are reasonably compliant to FEM analyses. However, the existing error among findings may be due to the effect of the existing adhesive layer among actuators and the base plate in empirical test. Similarly, it is not possible to attach the strain-gauges top and bottom of the notch exactly and this may be effective on the difference in results among empirical test and software analyses.

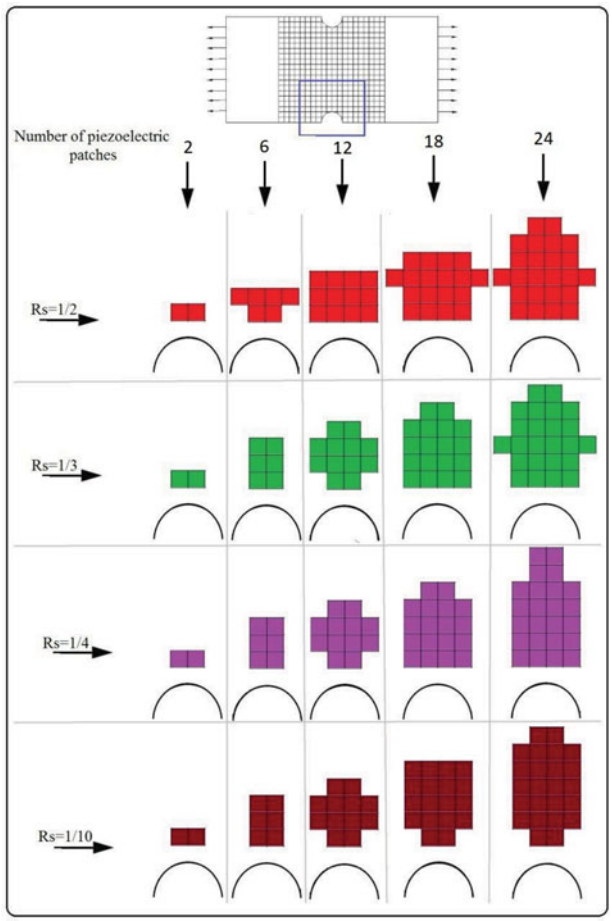

Figure 10. The best pattern of piezoelectric actuators placement around the notched for Rs < 1.

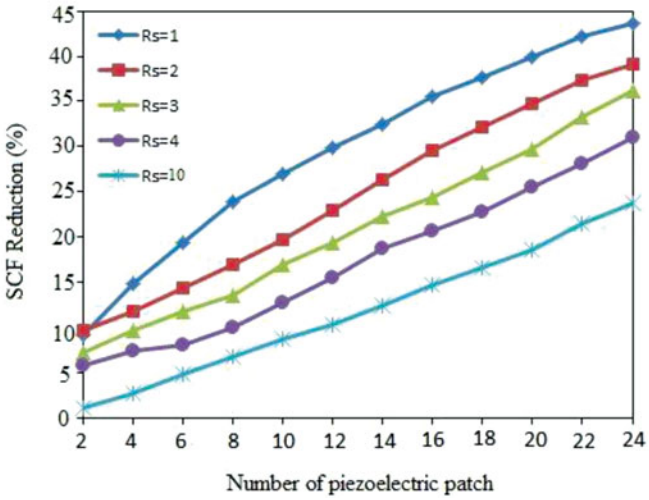

Figure 11. Effect of stiffness ratio on stress concentration reduction for Rs $\geq$ 1.

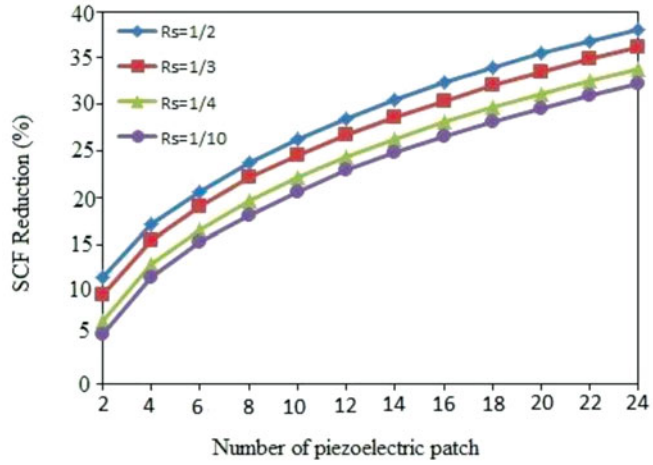

Figure 12. Effect of stiffness ratio on stress concentration reduction for Rs $<$ 1.

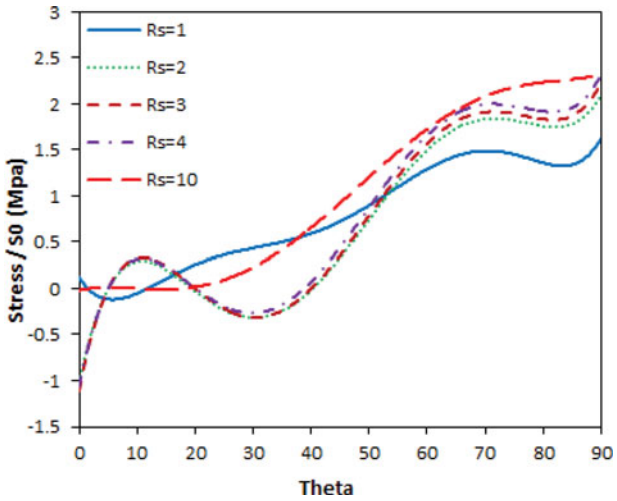

Figure 13. Longitudinal stress around the notched for Rs $\geq$ 1.

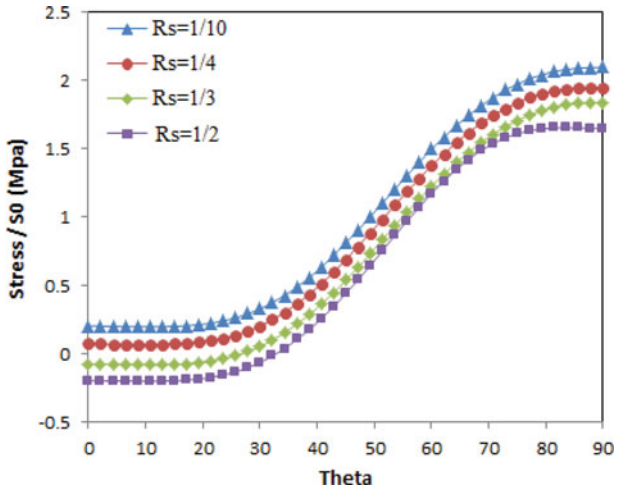

Figure 14. Longitudinal stress around the notched for Rs $<$ 1.

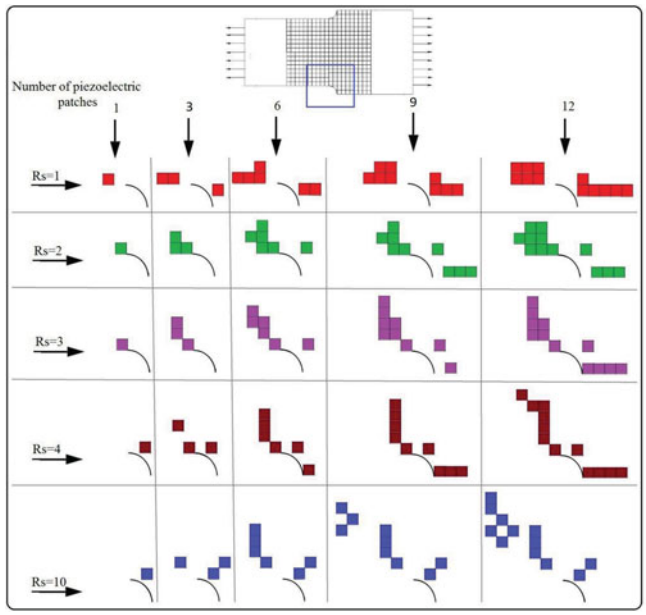

Figure 15. The best pattern of piezoelectric actuators placement around the filleted for Rs $\geq$ 1.

Table 1. Comparison of the results of analysis and experimental test for plate with hole.

Condition	Volt	Strain from FE	Strain from Test	Error
Rs = 2	0	46.6512×10^{-6}	45.742×10^{-6}	1.948%
	16.67 (E_0)	41.3062×10^{-6}	40.025×10^{-6}	3.1%
	33.34 ($2E_0$)	36.0444×10^{-6}	35.2895×10^{-6}	2.094%
	50.01 ($3E_0$)	30.7411×10^{-6}	29.856×10^{-6}	2.879%
	66.68 ($4E_0$)	25.4377×10^{-6}	24.965×10^{-6}	1.858%
	83.35 ($5E_0$)	20.1343×10^{-6}	19.871×10^{-6}	1.3%

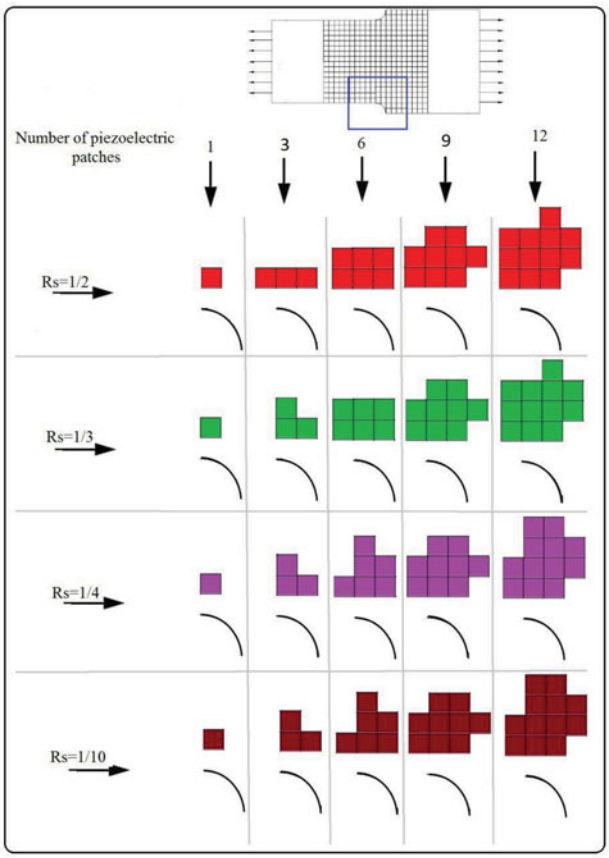

Figure 16. The best pattern of piezoelectric actuators placement around the filleted for Rs < 1.

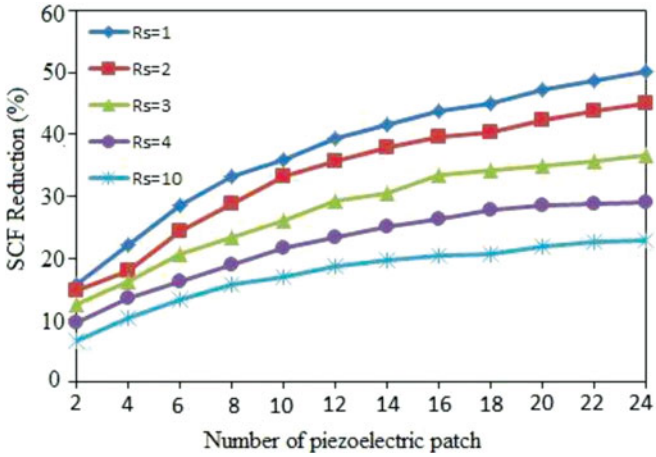

Figure 17. Effect of stiffness ratio on stress concentration reduction for Rs $\geq$ 1.

Table 2. Comparison of the results of analysis and experimental test for plate with notched.

Condition	Volt	Strain from FE	Strain from Test	Error
Rs = 2	0	46.5309×10^{-6}	45.233×10^{-6}	2.789%
	16.67 (E_0)	42.4047×10^{-6}	41.687×10^{-6}	1.692%
	33.34 ($2E_0$)	38.2784×10^{-6}	37.015×10^{-6}	3.3%
	50.01 ($3E_0$)	34.1522×10^{-6}	33.5621×10^{-6}	1.727%
	66.68 ($4E_0$)	30.0259×10^{-6}	29.25×10^{-6}	2.584%
	83.35 ($5E_0$)	25.8997×10^{-6}	24.865×10^{-6}	3.995%

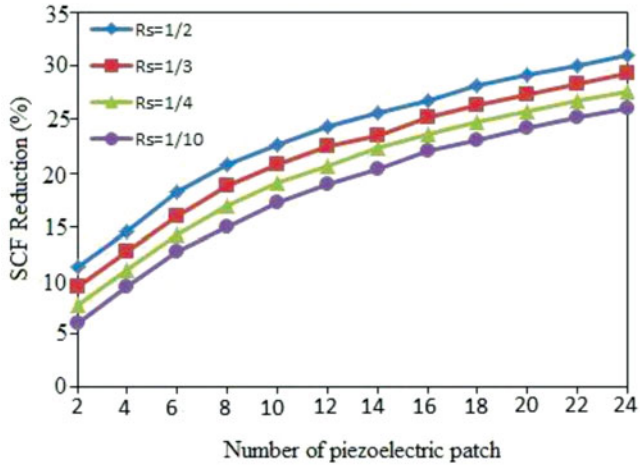

Figure 18. Effect of stiffness ratio on stress concentration reduction for Rs < 1.

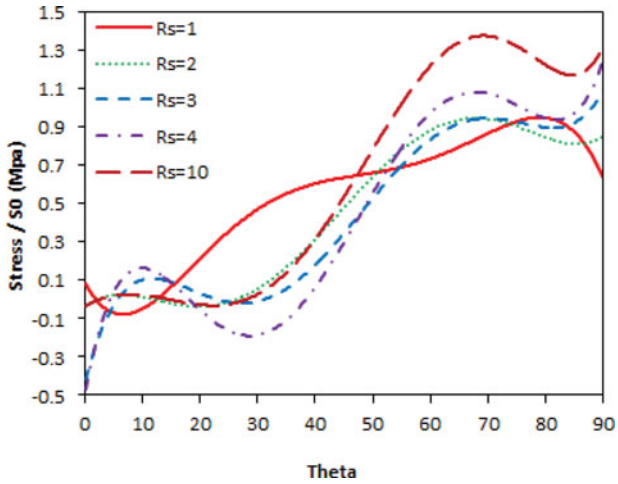

Figure 19. Longitudinal stress around the filleted for Rs $\geq$ 1.

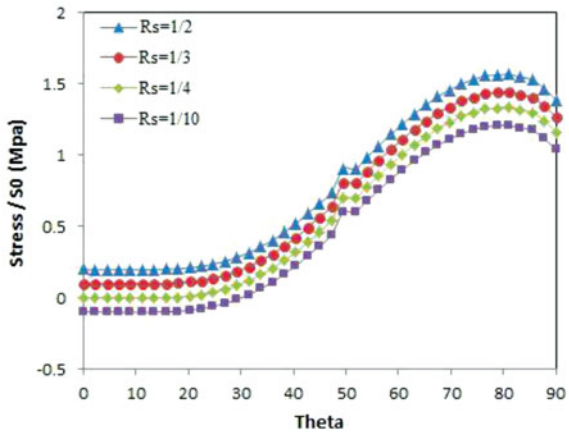

Figure 20. Longitudinal stress around the filleted for Rs < 1.

Table 3. Comparison of the results of analysis and experimental test for plate with filleted.

Condition	Volt	Strain from FE	Strain from test	Error
Rs = 2	0	29.3703×10^{-6}	28.986×10^{-6}	1.308%
	16.67 (E_0)	23.9928×10^{-6}	23.37×10^{-6}	2.595%
	33.34 ($2E_0$)	18.6153×10^{-6}	17.986×10^{-6}	3.38%
	50.01 ($3E_0$)	13.2377×10^{-6}	12.8956×10^{-6}	2.584%
	66.68 ($4E_0$)	7.86023×10^{-6}	7.652×10^{-6}	2.6491%
	83.35 ($5E_0$)	6.08679×10^{-6}	5.899×10^{-6}	3.085%

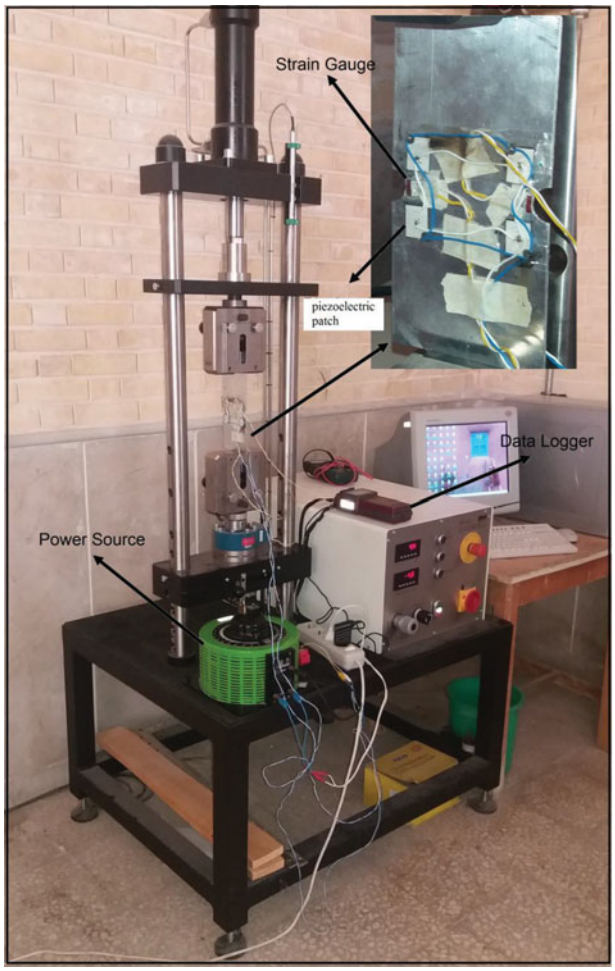

Figure 21. Schematic view of empirical tests.

7. Conclusion

We look for reduction of stress concentration factor in classic plates under tensile force in this article including plate with cavity, notched, and filleted plates. The purpose of this article is reduction of stress concentration factor in classic plate under tensile force including plate with hole, notched, and filleted plates using piezoelectric actuators. For this purpose, initially the ratio of stiffness is defined among piezoelectric actuator and host plate. We aim to find optimal models of piezoelectric actuators placement in these different ratios of stiffness to maximize reduction in stress concentration factor. A python code has been developed according to the PSO algorithm for FEM software to optimize piezoelectric actuators placement. The results indicate that piezoelectric actuators placement model is different in classic plates for stiffness ratios smaller and greater than one. Actuators are placed transversally toward the plate in stiffness ratios smaller than 1 and reduce stress in the plate, directly. However, at stiffness ratios greater than 1, they follow certain pattern in all classic plates and reduce stress indirectly by affecting the stress stream. The findings indicate that there is a certain pattern for piezoelectric placement in all classic plates. Three empirical tests have been utilized for placement site and different voltages were exerted to piezoelectric actuators to determine validation of tests. The results of the practical experiments show that there is a good agreement between the FEM and the laboratory test. The existing discrepancy is due to errors in the process of testing.

References

[1] M. I. Frecker, "Recent advances in optimization of smart structures and actuators," *J. Intell. Mater. Systems Struct.*, vol. 14, pp. 207–216, 2003. DOI: 10.1177/1045389X03031062.

[2] V. Gupta, M. Sharma, and N. Thakur, "Optimization criteria for optimal placement of piezoelectric sensors and actuators on a smart structure: a technical review," *J. Intell. Mater. Systems Struct.*, vol. 21, pp. 1227–1243, 2010. DOI: 10.1177/1045389X10381659.

[3] J. P. Amezquita-Sanchez, A. Dominguez-Gonzalez, R. Sedaghati, R. de Jesus Romero-Troncoso, and R. A. Osornio-Rios, "Vibration control on smart civil structures: A review," *Mech. Adv. Mater. Struct.*, vol. 21, pp. 23–38, 2014. DOI: 10.1080/15376494.2012.677103.

[4] T. Roy and D. Chakraborty, "Optimal vibration control of smart fiber reinforced composite shell structures using improved genetic algorithm," *J. Sound Vib.*, vol. 319, pp. 15–40, 2009. DOI: 10.1016/j.jsv.2008.05.037.

[5] A. R. Mehrabian and A. Yousefi-Koma, "A novel technique for optimal placement of piezoelectric actuators on smart structures," *J. Franklin Inst.*, vol. 348, pp. 12–23, 2011. DOI: 10.1016/j.jfranklin.2009.02.006.

[6] M. Dadfarnia, N. Jalili, Z. Liu, and D. M. Dawson, "An observer-based piezoelectric control of flexible Cartesian robot arms: theory and experiment," *Control Eng. Practice*, vol. 12, pp. 1041–1053, 2004. DOI: 10.1016/j.conengprac.2003.09.003.

[7] A. Mukherjee and A. S. Chaudhuri, "Active control of piezolaminated columns—exact solutions and experimental validation," *Smart Mater. Struct.*, vol. 14, pp. 475, 2005. DOI: 10.1088/0964-1726/14/4/003.

[8] P. A. Jadhav and K. M. Bajoria, "Free and forced vibration control of piezoelectric FGM plate subjected to electro-mechanical loading," *Smart Mater. Struct.*, vol. 22, pp. 065021, 2013. DOI: 10.1088/0964-1726/22/6/065021.

[9] X. Guo and J. Jiang, "Optimization of actuator placement in a truss-cored sandwich plate with independent modal space control," *Smart Mater. Struct.*, vol. 20, no. 11, pp. 115011, 2011. DOI: 10.1088/0964-1726/20/11/115011.

[10] K. Guo and Y. Xu, "Random vibration suppression of a truss core sandwich panel using independent modal resonant shunt and modal criterion," *Appl. Sci.*, vol. 7, no. 5, pp. 496, 2017. DOI: 10.3390/app7050496.

[11] R. Kumar, B. Mishra, and S. Jain, "Static and dynamic analysis of smart cylindrical shell," *Finite Elem. Anal. Des.*, vol. 45, pp. 13–24, 2008. DOI: 10.1016/j.finel.2008.07.005.

[12] P. Yao *et al.*, "Structural health monitoring of multi-spot welded joints using a lead zirconate titanate based active sensing approach," *Smart Mater. Struct.*, vol. 25, pp. 015031, 2015. DOI: 10.1088/0964-1726/25/1/015031.

[13] W. Tao, L. Shaopeng, S. Junhua, and L. Yourong, "Health monitoring of bolted joints using the time reversal method and piezoelectric transducers," *Smart Mater. Struct.*, vol. 25, pp. 025010, 2016. DOI: 10.1088/0964-1726/25/2/025010.

[14] N. Wu and Q. Wang, "An experimental study on the repair of a notched beam subjected to dynamic loading with piezoelectric patches," *Smart Mater. Struct.*, vol. 20, pp. 115023, 2011. DOI: 10.1088/0964-1726/20/11/115023.

[15] M. Kurata, X. Li, K. Fujita, and M. Yamaguchi, "Piezoelectric dynamic strain monitoring for detecting local seismic damage in steel buildings," *Smart Mater. Struct.*, vol. 22, pp. 115002, 2013. DOI: 10.1088/0964-1726/22/11/115002.

[16] V. M. F. Correia, C. M. M. Soares, and C. A. M. Soares, "Buckling optimization of composite laminated adaptive structures," *Compos. Struct.*, vol. 62, pp. 315–321, 2003. DOI: 10.1016/j.compstruct.2003.09.030.

[17] A. H. Daraji and J. M. Hale, "Active vibration reduction of a flexible structure bonded with optimised piezoelectric pairs using half and quarter chromosomes in genetic algorithms," *J. Phy.: Conf. Series*, vol. 382, pp. 012039, 2012.

[18] T. Fey *et al.*, "Mechanical and electrical strain response of a piezoelectric auxetic PZT lattice structure," *Smart Mater. Struct.*, vol. 25, pp. 015017, 2015. DOI: 10.1088/0964-1726/25/1/015017.

[19] Q. Nguyen, L. Tong, and Y. Gu, "Evolutionary piezoelectric actuators design optimisation for static shape control of smart plates," *Comput. Methods Appl. Mech. Eng.*, vol. 197, pp. 47–60, 2007. DOI: 10.1016/j.cma.2007.07.018.

[20] Q. Nguyen and L. Tong, "Voltage and evolutionary piezoelectric actuator design optimisation for static shape control of smart plate structures," *Mater. Des.*, vol. 28, pp. 387–399, 2007. DOI: 10.1016/j.matdes.2005.09.023.

[21] Q. Nguyen and L. Tong, "Shape control of smart composite plate with non-rectangular piezoelectric actuators," *Compos. Struct.*, vol. 66, pp. 207–214, 2004. DOI: 10.1016/j.compstruct.2004.04.039.

[22] Z. Kang and L. Tong, "Topology optimization-based distribution design of actuation voltage in static shape control of plates," *Comput. Struct.*, vol. 86, pp. 1885–1893, 2008. DOI: 10.1016/j.compstruc.2008.03.002.

[23] Z. Kang, X. Wang, and Z. Luo, "Topology optimization for static shape control of piezoelectric plates with penalization on intermediate actuation voltage," *J. Mech. Des.*, vol. 134, pp. 051006, 2012. DOI: 10.1115/1.4006527.

[24] P. K. Sensharma, M. J. Palantera, and R. T. Haftka, "Stress reduction in an isotropic plate with a hole by applied induced strains," *J. Intell. Mater. Systems Struct.*, vol. 4, pp. 509–518, 1993. DOI: 10.1177/1045389X9300400410.

[25] D. Shah, W. Chan, and S. Joshi, "Delamination detection and suppression in a composite laminate using piezoceramic layers," *Smart Mater. Struct.*, vol. 3, pp. 293, 1994. DOI: 10.1088/0964-1726/3/3/005.

[26] D. Shah, S. Joshi, and W. Chan, "Static structural response of plates with piezoceramic layers," *Smart Mater. Struct.*, vol. 2, pp. 2172, 1993. DOI: 10.1088/0964-1726/2/3/005.

[27] J. Jafari Fesharaki and G. Si, "Effect of stiffness ratio of piezoelectric patches and plate on stress concentration reduction in a plate with a hole," *Mech. Adv. Mater. Struct.*, vol. 24, pp. 1–32, 2016. DOI: 10.1080/15376494.2016.1139214.

[28] J. J. Fesharaki and S. Golabi, "A novel method to specify pattern recognition of actuators for stress reduction based on Particle swarm optimization method," *Smart Struct. Syst.*, vol. 17, pp. 725–742, 2016. DOI: 10.12989/sss.2016.17.5.725.

[29] J. Jafari Fesharaki and S. Golabi, "Optimum pattern of piezoelectric actuator placement for stress concentration reduction in a plate with a hole using particle swarm optimization algorithm," *Proc. Inst. Mech. Eng., Part C: J. Mech. Eng. Sci.*, vol. 229, pp. 614–628, 2015.

[30] J. Kennedy and R. Eberhart, "Particle swarm optimization. Neural Networks," *Proc. IEEE Int. Conf.*, vol. 4, pp. 1942–1948, 1995.